

Recent Trends in Microelectrode Array Technology for *In Vitro* Neural Interface Platform

Raeyoung Kim, Sunghoon Joo, Hyunjun Jung, Nari Hong and Yoonkey Nam

Received: 6 May 2014 / Revised: 30 May 2014 / Accepted: 3 June 2014
© The Korean Society of Medical & Biological Engineering and Springer 2014

Abstract

Microelectrode array (MEA) technology is a widely used platform for the study of *in vitro* neural networks as it can either record or stimulate neurons by accessing multiple sites of neural circuits simultaneously. Unlike intracellular recording techniques, MEAs form noninvasive interface with cells so that they provides relatively long time window for studying neural circuits. As the technology matured, there have been various engineering solutions to meet the requirements in diverse application areas of MEAs: High-density MEAs, high-throughput platforms, flexible electrodes, monitoring subthreshold activity, co-culture platforms, and surface micropatterning. The MEA technology has been applied to neural network analysis, drug screening and neural prostheses studies. In this paper, the MEA technology is reviewed and the future prospect is discussed.

Keywords Microelectrode array, Neural interface, Neural recording, Neural stimulation

INTRODUCTION

The electrophysiological characteristics of neural networks have long been studied to unravel the function of the brain. The electrical activities of neurons were recorded from a single-channel to network level and the related techniques helped to understand the underlying mechanisms of brain such as synaptic plasticity. The studies have been applied to various fields of neural engineering such as neural prostheses and neurological disorder treatments.

A planar microelectrode array (MEA) has become a popular experimental platform for electrophysiological studies of neural networks for *in vitro* models. An MEA was first introduced by Thomas *et al.* in 1972 as a new platform for studying cultured cardiac myocytes [1]. Since then, Pine and Gross reported successful experiments with cultured superior cervical ganglion cells [2] and ganglion cells from the snail *Helix pomatia* [3], respectively. In 1986, Wheeler and Novak reported the measurement of extracellular field potentials from brain slices and flexible MEAs were developed for elongated slice experiments [4, 5]. Since the early pioneering works, MEA technology has been applied to various neural network studies ranging from dissociated cell cultures to brain slices owing to its unique features: first, the MEA technology provides convenient spatiotemporal measurement platform. A few dozens of microelectrodes in one MEA chip provides simultaneous multiple signal recording. Second, an MEA provides a noninvasive cell-electrode interface that allows long-term recording and stimulation for days and weeks. The cultured neural network on MEA can maintain electrical activities more than a month by controlling the temperature and pH level of culture environment.

In this review, we introduce design principles and various MEAs for neural network studies. Then, we review the integration of MEA platform to microfluidic channel and surface micropatterning. Finally, we discuss the applications and future prospects of MEA technology.

WORKING PRINCIPLES

When neurons are cultured on an MEA, they adhere to the surface of an MEA and make direct contact with microelectrodes. MEAs record extracellular action potentials from active membranes of the neuron and microelectrodes can be also used to deliver electrical charges to stimulate

Raeyoung Kim, Sunghoon Joo, Hyunjun Jung, Nari Hong, Yoonkey Nam (✉)
Department of Bio and Brain Engineering, Korea Advanced Institute of
Science and Technology, Daejeon, Republic of Korea
Tel : +82-42-350-4322 / Fax : +82-42-350-4310
E-mail : ynam@kaist.ac.kr

neurons. The recording and stimulation were explained by volume conductor model for brain slices [6, 7], or by an electrical circuit model for cultured neurons [8-11]. In the circuit model, the interaction between the cell membrane and the non-electrode area is represented as a seal resistance. When action potentials are generated from neurons, extracellular ionic current flow occurs and creates extracellular voltage across the seal resistance. Microelectrodes detect the extracellular voltage which is in the range of tens to hundreds of microvolts. It was shown that the recording mode could be switched from extracellular recording to intracellular-like recording by artificially increasing the seal resistance [12]. For large cells, it was also shown that subthreshold activity could be measured by obtaining large seal resistance [13]. In case of stimulation, large seal resistance could dramatically decrease the current that is needed to activate the cellular membrane [14].

FABRICATION OF PLANAR-TYPE MEAs

As an MEA is aimed to interface with micrometer sized cells, a fabrication technique that provides design rules for micrometer scale features is essential. Since the first MEA was introduced in 1972 [1], an MEA has been made through microfabrication processes that are often used in semiconductor industry. To fabricate an MEA materials, for a substrate, conductor, insulator, microelectrodes, and culture chamber should be carefully selected. The choice of materials is closely related with the type of experiments that the MEA will be

used: primary cell culture, acute slice experiments, and organotypic slice culture. Some of the factors to be considered as follows: biocompatibility, optical transparency, substrate rigidity, and durability of insulation layers to cell culture conditions.

Metal patterning

Gold, platinum, or indium-tin oxide (ITO) is used for making metal patterns. Metal pattern is a base design for microelectrodes, conductor lines, and electrical contact pads for external instrumentation devices (Fig. 1a, 1b). The number of microelectrodes and inter space interval of microelectrodes are controlled by the pattern design. To realize these functions on a flat 2-dimensional surface, a thin film metal is deposited on a substrate (glass or silicon wafer) and patterned into 2-dimensional pattern (Fig. 2a, 2b). In case of gold or platinum, an additional metal layer such as titanium [15-18] or chromium [19, 20] is required to promote the adhesion between the glass substrate and metal. Heavily doped polysilicon was also used to prevent cracking and leakage of insulation layers [21]. For optical transparency, indium-tin oxide is used for conductor lines [22, 23]. To make a metal pattern, a thin metal layer is deposited onto the glass substrate using sputtering, thermal evaporation or e-beam evaporation. Then the desired pattern is made through photolithography followed by a wet or dry etching process. The density of electrodes is limited by line width, the size of the electrodes, and inter-electrode spacing. The width of the line is $3 \sim 8 \mu\text{m}$ and the thickness of the metal layer is $60 \sim 445 \text{ nm}$. In general, the number of electrodes is $32 \sim 60$ and

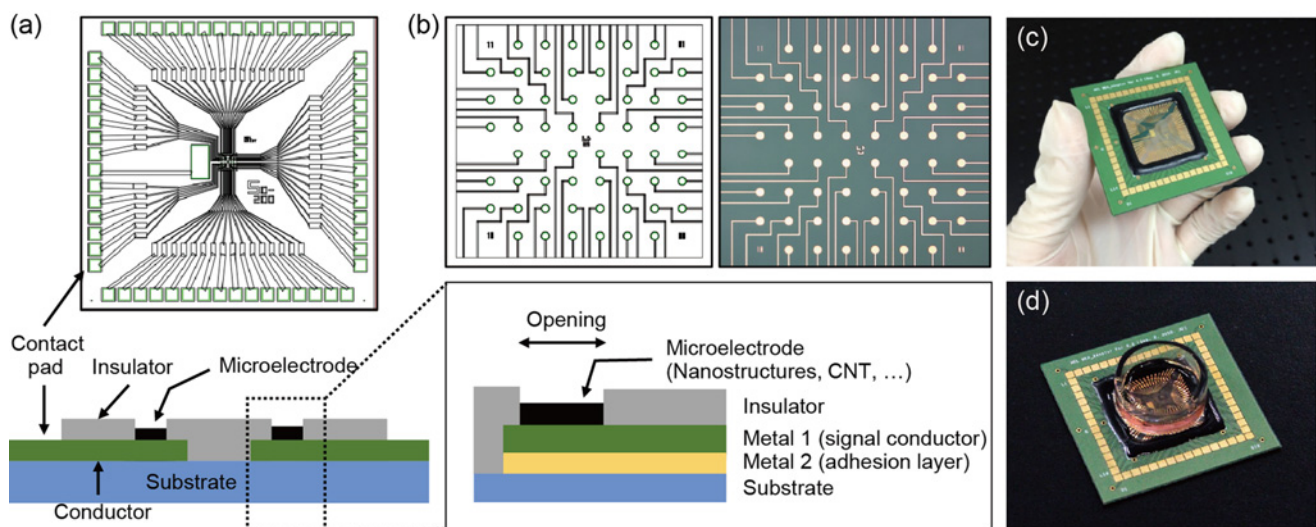


Fig. 1. Design and fabrication of an MEA. (a) A layout of an MEA with 60 electrodes including a reference electrode. (b) Microelectrode is defined by the size of the opening. Various materials and structures are added in the opening area. (c) A packaged MEA that can be connected with external connectors to electronic instruments. (d) A small cell culture chamber is defined by installing a glass ring surrounding the electrodes. Insulator serves as a cell culture substrate (Photos were provided by Neural Engineering Laboratory in KAIST, South Korea).

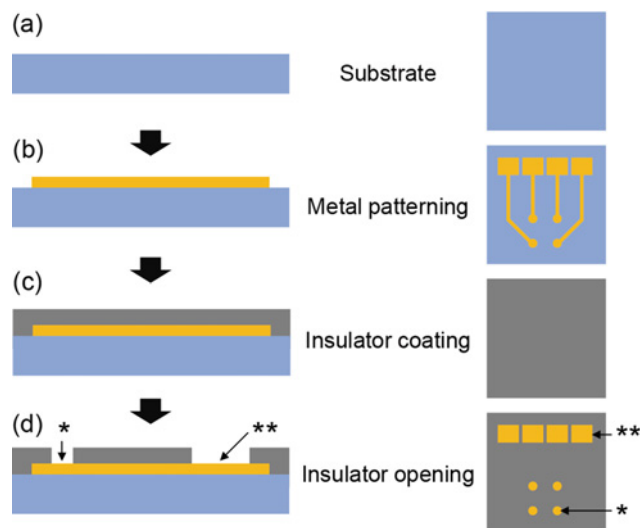


Fig. 2. MEAs share common fabrication steps: metal patterning, insulation, and electrode opening.

the inter-electrode spacing is 100 ~ 250 μm , while a 512 electrode MEA was also reported [23]. The layout and the spacing of the electrodes depend on the application and they are limited by the fabrication methods used for metal patterning.

Insulation

To make a microelectrode structure, conductor lines need to be passivated by an insulator (Fig. 2c). A good insulator should minimize signal crosstalk and signal attenuation. As an MEA is operated with aqueous solutions containing abundant ions, an inert insulation layer is required to sustain any degradation under ionic attacks. Various materials have been tried for insulation. Silicon dioxide [2], silicon nitride [23-26], and ONO ($\text{SiO}_2\text{-Si}_3\text{N}_4\text{-SiO}_2$ composite) [21, 27-29] have been used. To deposit inorganic layers chemical vapor deposition (CVD) such as plasma-enhanced CVD or low-pressure CVD is used. Typical thickness for the inorganic materials is 500 ~ 3000 nm. Thicker insulation layers (2 ~ 5 μm) are obtained with the polymers. Polymers such as polysiloxane resin [30], SU-8 [20, 31], polyimide [4, 15, 16, 32], acrylic imide film [22], polydimethylsiloxane (PDMS) [33-35] and parylene [36] are also used. Recently, flexible MEAs have been reported for better interaction between tissues and MEAs [35].

Opening of microelectrodes

Following the insulation of a metal pattern, via-holes are formed at both ends of the metal line to define microelectrodes and contact pads (Fig. 2d). Photolithography is used to impose the layout of microelectrodes and contact pads on the insulator and the insulator is selectively etched to

make via-holes. In case of the microelectrode, the size of the opening determines the size of the electrode. For etching SiO_2 , hydrofluoric acid buffer solution was used [2]. To etch Si_3N_4 , reactive etching with SF_6 [23] and fluoride ions [24] were used. CF_4 and CHF_3 were used for reactive ion etching of ONO layer opening [27]. In case of photo-definable polymers such as SU-8, exposure to UV and development made the holes [31]. Parylene [36] and polyimide [16] were etched with oxygen plasma. A via-hole on a PDMS layer was formed using a SU-8 lift-off process [33].

Packaging

To read electrical voltage at the microelectrode, MEAs need to be connected with external read-out circuitry (e.g. amplifier and filter). An MEA chip can be designed large (~ 2 inch \times 2 inch) and the contact pads are directly connected with the headstage amplifiers. In this way, there is no need for a packaging process. However, making a large chip significantly reduces the number of chips that can be batch-processed per a wafer (4 inch or 8 inch). An alternative way is to design a small chip (~ 1 inch \times 1 inch) and package each chip with a printed-circuit board adaptor that connects the glass MEA chip with the read-out circuitry (Fig. 1c). The connection between contact pads and the PCB board is implemented by wire-bonding with gold wires [18] or conductive glues [31]. If the number of electrodes scales up to a few thousands, wiring individual electrodes become cumbersome and very large-scale integrated circuit (VLSI) design techniques are required to reduce the number of external connections.

Culture chamber

To grow cells on an MEA, a glass or Teflon ring that can hold cell culture medium is installed. The ring should be securely attached on the MEA surface so that the medium will not leak (Fig. 1d). Since the ring can only hold a small amount of culture medium (1 ~ 2 ml), it is often necessary to prevent the evaporation by installing transparent gas permeable and water impermeable FEP (fluorinated ethylene-propylene) membrane [37]. This is especially useful when the recording is performed in a low humidity atmosphere or handling a extremely small volume [38].

ELECTRODE MATERIALS

The recording performance of MEAs is mainly determined by the impedance of the microelectrode. The impedance is closely related to the electrode thermal noise and reducing the noise level is possible by lowering the impedance [9, 25, 39]. The size of the microelectrode ranges from 5 μm to 50 μm in diameter and the surface area is too small to

provide sufficiently low impedance. Thus, the surface of the microelectrode is modified with conductive materials to increase the effective surface area, which would lower the impedance.

Metal nanostructures have been added on an MEA using platinum or gold. Platinum black is a classic example for the surface modification of the microelectrodes on an MEA [2]. Porous platinum black structure can be obtained by a simple electrochemical deposition method. It has porous structure which is effective for impedance reduction [4, 15, 23, 40]. The plantinized microelectrodes, whose size was $5 \sim 25 \mu\text{m}$, had impedance in the range of $12 \sim 400 \text{ k}\Omega$ at 1 kHz and the noise level was $2 \sim 5 \mu\text{V}_{\text{rms}}$. However, the structure is mechanically fragile so that it could be damaged during the usage. Recently, mechanically stable nanoporous platinum microelectrodes were reported to overcome this disadvantage [41]. To fabricate a mechanically strong nanoporous platinum structures Chung and coworkers used a micelle-add platinum solution for electrodeposition (Fig. 3a). As a result, the constructed platinum nanostructure endured normal force from diamond indenter without any peel off or demolishing. The impedance value was $2.4 \text{ k}\Omega$ at 1.17 kHz (size: $45 \mu\text{m}$ in diameter). Gold is another classic electrode material due to its high conductivity, biocompatibility, and chemical stability [3]. Various gold nanostructures have been reported using different fabrication methods. Using electrochemical deposition method, nanoflake (Fig. 3b) [19], nanograin (Fig. 3c) [18] and fuzzy gold [42] structures were constructed. Although gold did not form a porous structure, each nanostructure formed rough surfaces to increase the surface area. The impedance of nanoflake microelectrode was $26.7 \text{ k}\Omega$ at 1 kHz (size: $15 \mu\text{m}$ in diameter), and the noise level was $3.5 \mu\text{V}_{\text{rms}}$. For nanograin and fuzzy gold, grain structures enlarged the surface area of microelectrodes and resulted in low level of impedances which were $100 \text{ k}\Omega$ and $126 \text{ k}\Omega$ for $20 \mu\text{m}$ and $10 \mu\text{m}$ sized microelectrodes at 1 kHz, respectively. Moreover, mechanical stability was better than platinum black [19]. Using a top-down method, gold nanopillar was fabricated using aluminum oxide template [27] and nanoporous gold was formed through repeated annealing process at high temperature [20]. The noise level of $10 \mu\text{m}$ of nanopillar microelectrodes was $6.7 \mu\text{V}_{\text{rms}}$ and the impedance of nanoporous gold was $30 \text{ k}\Omega$ at 1 kHz with $32 \mu\text{m}$ sized microelectrodes whose noise level was $5.5 \mu\text{V}_{\text{rms}}$. To increase the cell-electrode contact with low electrode impedance, a microelectrode with small opening and large surface area ('nanocavity microelectrode') was fabricated and demonstrated with HL-1 cells [43]. TiN was deposited on gold electrodes by reactive sputtering in an argon/nitrogen atmosphere and its nano-scale columnar structure reduced the electrode impedance dramatically [24].

Carbon nano tubes (CNTs) showed high potential as

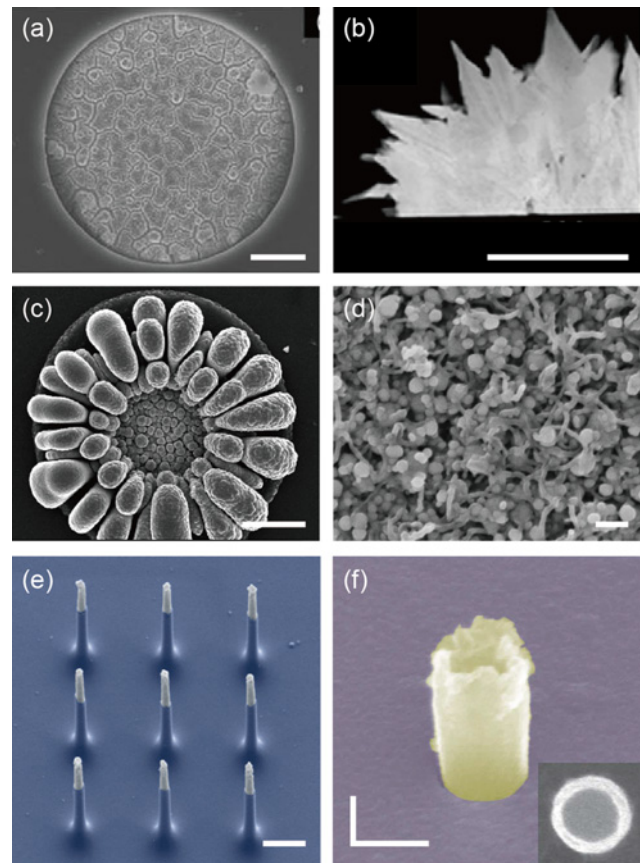


Fig. 3. Various types of micro/nano structured microelectrodes. (a) nanoporous platinum, (b) gold nanoflake, (c) gold nanograin, (d) carbon nanotube, (e) silicon nanowire, and (f) iridium oxide nanotube (scale bar: (a) $10 \mu\text{m}$, (b) $1 \mu\text{m}$, (c) $5 \mu\text{m}$, (d) 200 nm , (e) $1 \mu\text{m}$, (f) $2 \mu\text{m}/200 \text{ nm}$). Figures reprinted with permission from (a) [41], Copyright 2010 American Chemical Society; (b) [19], Copyright 2010 IOP Publishing; (c) [18], Copyright 2013 WILEY-VCH Verlag GmbH & Co. KGaA, Weinheim; (d) [22], Copyright 2013 Elsevier; (e) [54], Copyright 2012 NPG; (f) [55], Copyright 2014 NPG.

microelectrode material. They effectively increased the surface roughness of microelectrodes, which results in recording performance improvements. Through chemical vapor deposition (CVD), CNTs were synthesized on microelectrodes. Nickel layer was deposited on titanium nitride microelectrode and used as catalyst sites for CNT growth [26]. Impedance of CNT microelectrode (size: $80 \mu\text{m}$ in diameter) was $10 \text{ k}\Omega$ at 1 kHz, the noise level was $7 \mu\text{V}_{\text{rms}}$, and the signal to noise ratio (SNR) was as high as 135. Harris and coworkers used iron as a catalyst and grew protruding CNT microelectrodes with the charge injection limit reaching $1 \sim 1.6 \text{ mC}/\text{cm}^2$ [21]. Furthermore, electroplating [22, 44] and microcontact printing method [45] were also used to deposit multiwall CNTs (Fig. 3d). The multiwall CNT structure provided higher SNR, which was approximately 130, compared to normal titanium nitride microelectrode in similar size ($30 \sim 40 \mu\text{m}$ in diameter). Boron-doped nanocrystalline diamond was also

fabricated into an MEA format with various insulation materials (SU8, ONO, and nanocrystalline)[46].

Conductive polymer is also a promising material for microelectrodes since it provides low impedance and versatile platform for additional material conjugation. Representative conductive polymers applied to MEAs are poly(3,4-ethylenedioxythiophene) (PEDOT) and polypyrrole. PEDOT or polypyrrole modified microelectrodes showed low level of impedance [47-49]. PEDOT deposited microelectrode revealed impedance 5.7 ~ 20 folds decrease, resulting in background noise reduction from 106 ~ 116 μV to 35 ~ 51 μV [48]. In addition, CNT [50, 51], graphene [52] or biomolecules [47] could be conjugated into conductive polymer structures and improved the neural recording performance. CNT and graphene increased the charge injection capacity for neural stimulation up to 202.9 mC/cm^2 [51] and 242.1 mC/cm^2 [52], whereas normal platinum electrodes showed 1.4 mC/cm^2 .

Nanowire electrodes were fabricated on microelectrodes in order to control the electrode-membrane interface. Following the cell-penetration effect of nanowires on mammalian cells [53], a few groups attempted to apply the phenomenon to the MEA design. Park and coworkers made an MEA with vertical silicon nanowires (Fig. 3e) [54]. Vertical silicon nanowires were fabricated through nanofabrication technique, which is widely adopted for integrated silicon electronic circuit production. Each microelectrode had nine nanowires on its surface, whose diameter and length were 150 nm and 3 μm , respectively. Using this type of nanowire-MEAs, they recorded evoked action potentials of rat cortical neuron, whose SNR was more than 100. Cui and coworkers reported vertical nanopillar or nanotube electrodes for transient intracellular recording (Fig. 3f) [17]. For nanopillar formation, holes were etched on passivation layer by focused ion beam (FIB) milling and platinum was deposited into the holes through FIB-assisted platinum deposition. The action potentials of cultured cardiomyocytes were recorded, which SNR was in the range of 4.5 ~ 9. By applying 2.5 V of voltage pulses, transient intracellular signals were recorded, which SNR was increases to 590. Recently, they reported iridium oxide nanotubes that elongated the duration of transient intracellular recording up to one hour [55].

Surface modification of electrode surfaces is of interest as cell-adhesive biomolecules could be chemically linked to modulate cell-electrode coupling. Although the chemical modification can affect the electrode impedances, it would be beneficial to biofunctionalize the electrodes for cell-electrode coupling [56]. Spira and coworkers used a protein linking chemistry (3-aminopropyltriethoxysilane and 4-maleimidobutyric acid sulfo-N-succinimidyl ester) to immobilize cysteine terminated RGD peptides to gold-spine electrodes [13]. Nam and coworkers utilized electrochemical deposition technique to synthesis polydopamine on microelectrodes

[57]. They showed that incorporation of poly-D-lysine or RGD peptides was possible on the electrodes.

ULTRA-HIGH DENSITY CMOS-TYPE MEAs

High spatial resolution recording is desirable for the cellular level studies of neural circuits. To increase a spatial resolution and electrode counts, an ultra-high density MEA with thousands of channels was developed using the state-of-the-art VLSI circuit design technology. VLSI circuit design utilizes Complementary-Metal-Oxide-Semiconductor (CMOS) fabrication processes to integrate millions of circuit elements on a silicon chip. Using the same design rules, CMOS-type MEAs were designed to integrate dense microelectrodes, amplifiers, filters, stimulation buffer, multiplexer, digital logic circuits, and analog-to-digital converter circuitry on a same silicon substrate. Multi-layer CMOS fabrication processes allowed to increase the electrode density and on-chip multiplexing technique made it possible to access thousands of electrodes using the reduced number of output channels. The channel selection capability made it possible to select a set of electrodes that were of interest. The high data rate transfer, electrode addressing, and timing control are programmed through FPGA platform and high-speed data bus (USB or PCI) was used to transfer the data to PC. FPGA became an essential interface system to build the real-time data acquisition for CMOS-type MEAs.

The CMOS type MEA is fabricated through two steps: VLSI circuit fabrication on a chip and the microelectrode array fabrication process. An VLSI circuit that contains amplifier, filter, analog-to-digital converter, multiplexer, and digital circuits is fabricated by a commercial foundry service and a dedicated area for a microelectrode array is left for post-process. During the post-processing, electrodes are fabricated and passivation layers are added to protect the active circuitry from electrolytes.

Several research groups have reported CMOS-type MEAs with ultra-high density electrode counts. Fromherz and coworkers used 0.5- μm CMOS process to make a 128 \times 128 electrode MEA (sensor area: 1 mm \times 1 mm) [58] (Fig. 4a). They made oxide-semiconductor field-effect transistor array with a pitch of 7.8 μm \times 7.8 μm . On a CMOS chip, they patterned metal electrode patterns and contact pads using Ti and Pt and the stack of TiO_2 and ZrO_2 (40 nm) was sputtered to obtain high dielectric constant (Fig. 4b). The sensor chip had 128 \times 128 pixel array, 128 channel readout amplifiers, 8-to-1 multiplexer, and address decoder. They achieved the full frame rate of 2 kps for recording from the entire array. The power consumption was 656 mW, which required the regulation of the chip temperature for biological experiments. An action potential from a snail neuron was successfully recorded. This group reported a next version with improved noise level (40 ~ 80 μV) and faster frame rate (6 kHz) and applied to study

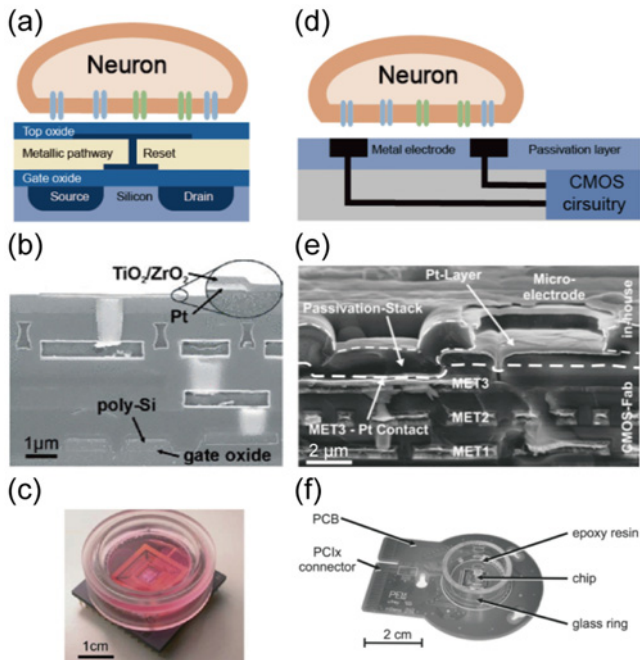


Fig. 4. Examples of CMOS-type MEAs. Multi-transistor array developed by Fromherz and coworkers used the oxide layer as a sensing element (a). The device structure (b) and a packaged chip (c) are shown (Reprinted with permission from [108], Copyright 2004 Springer). Microelectrode array integrated with CMOS circuitry developed by Hierleman and coworkers used metal electrode as a sensing element (d). The device structure (e) and a packaged chip (f) are shown (Reprinted with permission from [67], Copyright 2010 IEEE).

the signal propagations in retinal ganglion networks [59, 60]. A same technology was used to design a multicapacitor array (400 sites, $50 \mu\text{m} \times 50 \mu\text{m}$) for electrical stimulation of retinal slices [61].

Berdondini and coworkers used $0.35 \mu\text{m}$ CMOS process for a 64×64 electrode MEA (active area: $2.67 \text{ mm} \times 2.67 \text{ mm}$) [62, 63]. They used gold electrode with the size of $21 \mu\text{m} \times 21 \mu\text{m}$ spaced by $21 \mu\text{m}$. The CMOS chip had Al electrodes so that biocompatible gold microelectrodes were formed on Al using electroless plating [64]. Silicon oxide from the CMOS foundry service was used as it is to protect the circuitry during cell culture experiments. In their design, electrodes, amplifier, addressing decoder, and multiplexers were integrated on a sensor chip. Analog-to-digital conversion was done with off-chip ADCs on a FPGA board. To handle a large data rate, camera link with frame grabber was used. Full frame rate was 7.8 kHz for 4096 channels and input-referred noise level was $11 \mu\text{V}_{\text{rms}}$. The power consumption was 132 mW and it did not raise the temperature of cell culture media significantly. This chip has been interfaced with primary neuronal cultures derived from rat hippocampus or cortex [62], acute brain slices [65], and mouse retinal tissues [66].

Hierleman and coworkers used $0.6 \mu\text{m}$ CMOS process for 11011 electrode MEA system (sensor area: $2.0 \text{ mm} \times 1.75 \text{ mm}$) with the simultaneous recording and stimulation capacity of 126 channels [67, 68] (Fig. 4d). Each electrode had the size of $7 \mu\text{m}$ in diameter and electrodes were spaced by $18 \mu\text{m}$. After adding $0.5 \mu\text{m}$ thick SiO_2 layer for passivating CMOS layer, they patterned Pt for electrodes and a thick passivation layer ($1.6 \mu\text{m}$) was added by stacking SiO_2 and Si_3N_4 layers alternatively. To lower the electrode impedance, platinum black was deposited on the Pt electrodes (Fig. 4e). A sensor chip integrated row decoder, multiplexers, 126 readout/stimulation channels, 16 ADCs, 2 DACs, and digital control circuitry. The chip was interfaced with FPGA board to control the data acquisition and real-time feedback controls. Each channel could be sampled at 20 kHz . The selection of 126 channels from 11011 electrodes was configurable. The input-referred noise level was $2.4 \mu\text{V}_{\text{rms}}$ ($1 \text{ Hz} - 100 \text{ kHz}$) and the power consumption was 135 mW . This chip was used to investigate the extracellular electrical field in Parasagittal cerebellar slices [68]. Real-time spike detection and closed-loop feedback stimulation were demonstrated with the FPGA system [69]. More recently, Bakkum and coworkers combined the on-chip electrical stimulation capability and high-resolution recordings to map the propagation of action potentials in a single cortical neuron [70]. This group recently reported an upgraded system that is capable of recording 1024 channels from 26400 electrodes. Using the $0.35 \mu\text{m}$ CMOS process, power consumption was reduced to 75 mW and input referred noise level was $2.4 \mu\text{V}_{\text{rms}}$ [71].

MICROFLUIDIC MEAs

Microfluidic technology based on PDMS devices has been proposed as a novel cell culture platform as the technology can provide a methodology to create *in vivo* like microenvironments for cultured neurons [72]. A two-compartment PDMS device has become a popular cell culture platform for growing neurons [73]. The concept of the design was originally developed by Campenot [74] and implemented into a microfluidic platform by Jeon and others (Fig. 5a). The device is composed of two or more compartments for cell seeding and several microchannels connected the compartments. The size of channels (cross-section: $3 \mu\text{m} \times 10 \mu\text{m}$) was demonstrated that it was too small to permit somata to migrate into the channels and only axons could extend out to the other compartment [73]. Using these devices, microfluidic devices were successfully demonstrated for separating axons from somata and dendrites [73], neuron-astroglia co-culture system [75], or constructing a functional circuit with two different populations of neurons from different brain regions [76]. These microfluidic channel devices that allow the compartmentalization

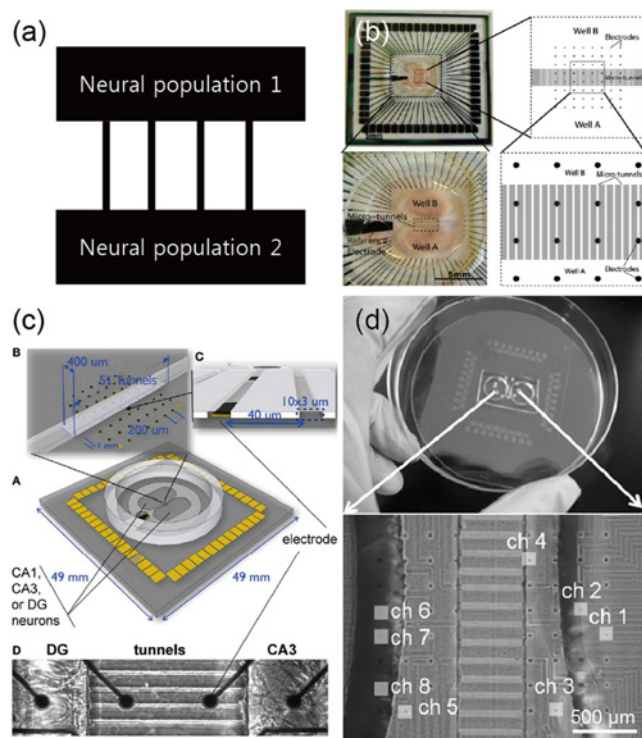


Fig. 5. Application of microfluidic devices to the MEA platform. (a) Two-population neural network model inspired from Jeon *et al.* [73]. (b) Integration of two-compartment devices with 60-channel MEAs. Electrodes were located in micro-tunnels to record action potentials from axons connecting two neural populations (Reprinted with permission from [79], Copyright 2011 IOP Publishing). (c) Reconstruction of DG-CA3 networks using microfluidic devices (Reprinted with permission from [80], Copyright 2013 Brewer, Boehler, Leondopulos, Pan, Alagapan, DeMarse and Wheeler). (d) Co-culture of P19-derived neurons and mouse cortical neurons (Reprinted with permission from [84], Copyright 2011 Elsevier).

of neurons and fluidic environment have been applied to an MEA in later studies.

Axon signal recording and analysis was possible through microfluidic channel integration to MEA platform. Because axonal growth is only possible in microchannels between compartments, the small signals from isolated bundles of axons can be recorded and the propagation velocity through the bundles was measured by aligning each microchannel on electrodes [77]. Dworak and Wheeler showed that microchannels had signal boosting effect due to the high end-to-end resistance of channels. They were able to record relatively large signals ($\sim 200 \mu\text{V}$) from isolated axons, which was difficult to record using a conventional MEA. Mepivacaine, a sodium channel blocker, resulted in the alteration of mean spiking rate and conduction velocity [77]. Claverol-Tinture and coworkers showed that axons growing in a microchannel could be approached as a loose-patch configuration, and they were able to measure spikes from axons [78]. Nam and coworkers demonstrated a long-term recording of cultured

neurons in microchannel-environments for up to five weeks [38].

Microfluidic compartmental devices were also utilized for constructing networks of neural populations. Wheeler and coworkers utilized a sequential cell plating method that lead to the filling of microchannels with axons from the firstly plated wells. They reported that 84% of the measured spikes were propagating from the first well to the second well, which indicated the establishment of unidirectional connections between two neuronal populations (Fig. 5b) [79]. Unidirectional connectivity between two wells was also verified from burst propagation. To understand the tri-synaptic network of the hippocampal formation pathway from the dentategyrus (DG) to the CA3 and CA1, pairs of the pathways were reconstructed with microfabricated device divided into two compartments (Fig. 5c) [80]. In DG-CA3 co-culture case, spikes from DG axons propagated preferentially to CA3 neurons without external inputs and the burst dynamics of each compartment were different from DG-DG or CA3-CA3 culture cases. Voldman and coworkers controlled the axonal growth by switching on or off the high frequency ($< 100 \text{ kHz}$) electric field in the microchannels [81]. It allowed them to form a neural circuit of three neuronal populations. In cortical-thalamic co-culture system, synchronized network bursts initiated in cortical compartment and propagated to the thalamic compartment, while there was no preferred direction in cortical-cortical co-culture systems [82]. Synaptic receptor antagonist in cortical compartment influenced the bursting in thalamic compartment. The integration systems were used to control the connectivity for developing *in vitro* models of patterned neuronal networks and to characterize electrical activity of each compartment and interaction between them [83]. Functional connectivity maps of each compartment using cross-correlation based techniques demonstrated that functional connections not only within each compartment but also with each other were formed. Stem cell-derived neurons and primary neurons were cultured in each compartment of devices to study the interactions between the two neural networks (Fig. 5d) [84]. From the spontaneous activities in co-cultured system recorded by an MEA, periodic synchronized bursts were observed in both compartments for two weeks but the activity profiles from compartment of P19-derived neurons were different from those from monoculture case. Consequently, the functional interactions between two types of neurons were demonstrated.

SURFACE-MICROPATTERNED MEAs

Designed neural network via several surface micropatterning approaches provided opportunities to study the relationship between functional properties and geometry of neuronal

networks [85]. The position of cell body, the direction of axon and dendrites could be controlled by restricting the

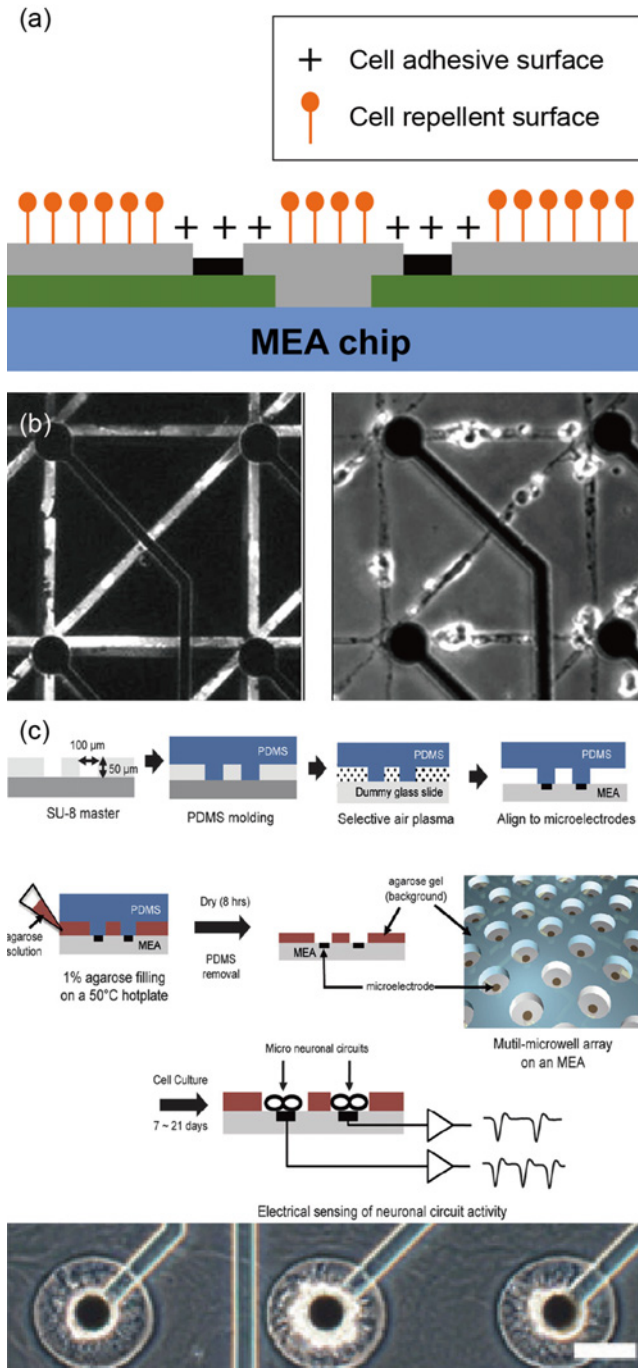


Fig. 6. Surface micropatterning of MEAs. (a) Surface of an MEA can be patterned to either promote or prohibit neuronal growth using appropriate biomolecules and surface biofunctionalization methods. (b) Microcontact printing of cell-adhesive biomolecules on MEAs and the formation of patterned neuronal networks (Reprinted with permission from [89], Copyright 2011 Elsevier). (c) Cell-repellent agarose hydrogel was microstructured using micro-molding in capillary technique ([97] – Reproduced by permission of The Royal Society of Chemistry).

adhesion and growth of neurons on an MEA (Fig. 6a). An MEA surface is patterned into cell-adhesive and cell-prohibitive areas using physical or chemical micropatterning techniques. One of the earliest examples was done by patterning polylysine lines by a lift-off technique and recorded electrical signal from cultured hippocampal neural network for four weeks [15]. To do a lift-off technique on an MEA, the MEA chip itself need to go through photolithography process (photoresist spin coating, baking, UV exposure, and development) and cell adhesive molecules were patterned in a few micrometer scale [86-88]. Microcontact printing which uses a PDMS stamp to print micropatterns of biomolecules on a surface was more convenient to apply chemical patterning on MEAs (Fig. 6b). There were many reports that succeeded in printing cell-adhesive molecules on an MEA and recorded from patterned neuronal networks [16, 29, 56, 89-92]. To facilitate the immobilization of biomolecules and the MEA surfaces, surface modification schemes using alkanethiolate [16], organosilane [56, 86], or polydopamine [57, 93] has been reported. Recently, Suzuki *et al.* used a different approach to pattern an MEA. They activated polymeric MEA surface using UV ozone and covalently linked polylysine on the entire surface. Then, vacuum UV was selectively irradiated on the MEA surface to modify the cell-adhesiveness of polylysine so that neuronal patterning was possible [94].

Physical structures are also used to pattern MEA surfaces. Thin layer of polyimide was patterned on an MEA, and it was the cast for designing neural network [95]. Recently, agarose hydrogel, which is known to be a perfect surface to inhibit neuronal attachment, was patterned on an MEA. Jimbo and coworkers devised a photothermal etching process to construct microtunnels in agarose hydrogel layer. They successfully demonstrated the construction of unidirectional neural circuits on an MEA by controlling axonal outgrowth *in situ* [96]. Nam and coworkers used soft-lithography to construct agarose microwell arrays on an MEA (Fig. 6c) [97]. As discussed in previous section, microfluidic channel devices are actively used with an MEA to construct neural circuits on an MEA.

OPTICAL INTERFACE WITH MEAs

Optical stimulation and recording techniques have been used as a complementary method to interrogate neural circuits on an MEA. The transparency of the glass substrate allows an MEA to be easily interfaced with optical microscopes. For optical transparency, glass substrates, and a transparent conductor (*e.g.* indium-tin oxide) are used to fabricate an MEA [22, 23]. In this case, the entire chip surface is optically accessible through an inverted microscope setup, except the small area covered by microelectrodes. Calcium

Table 1. Examples of MEA specifications.

Year	Ref.	Electrode material	No. electrodes	Size* (μm)	$ Z $ (k Ω), kHz	Conductor (thic.: nm)	Insulator (thic.: μm)	Substrate	<i>In vitro</i> testing**
2004	[23]	Pt black	512	5 (dia)	200	ITO (150)	Si ₃ N ₄ (2)	Glass	(r) Retinal slices
2006	[21]	MWCNT	36 (6 \times 6)	30 (sq)	3 ~ 4	Doped polySI (500)	ONO (2.25)	Glass	(s) Rat neurons (h)
2007	[26]	MWCNT	60	80 (dia)	1.1 ~ 10	TiN (80)	Si ₃ N ₄ (0.3)	Si wafer	(r) Rat neurons (c)
2007	[29]	Pt black	32 (4 \times 8)	10 (sq)	112	Au (300)	ONO (NA)	Glass	(r/s) Rat neurons (h)
2009	[62]	Au	4096	21 (sq)	NA	Al	SiO ₂	CMOS	(r) Rat neurons (h)
2009	[67]	PtBK	11011	7 (dia)	NA	Pt (200)	SiO ₂ -Si ₃ N ₄ (1.6)	CMOS	(r/s) Rat neurons (h) Brain slice
2010	[13]	Au spine	62	NA	NA	Au (45 ~ 65)	SiO ₂ (0.3)	Glass	(r) Aplysia neuron
2010	[19]	Au nanoflake	60	5 ~ 50 (dia)	12 ~ 150	Au (200)	Si ₃ N ₄	Glass	(r) Rat neurons (h)
2010	[20]	Au nanoporous	64 (8 \times 8)	32 (dia)	30	Au (120)	SU-8 (2)	Glass	(r) Brain slice
2011	[35]	PEDOT:PSS	60	120 (dia)	400 ~ 1000	PEDOT:PSS	PDMS	PDMS	(r) Brain slice
2011	[27]	Au nanopillar	NA	15 (dia)	NA	Au (200)	ONO (0.8)	Si wafer	(r) HL-1 cell
2012	[54]	Si nanowire	16 (4 \times 4)	0.15 (dia) 3 (H), 3 \times 3	NA	Doped Si	Al ₂ O ₃ (0.1)	Si wafer	(r) Rat neurons (h)
2012	[84]	Pt black	64	30 (sq)	100	ITO	NA	Glass	(r) Mouse neurons (c) P19-derived neurons
2012	[17]	Pt nanopillar	16 (4 \times 4)	0.15 (dia), 1.5 (H), 3 \times 3	6000	Pt (100)	Si ₃ N ₄ /SiO ₂ (0.35)	Quartz	(r) Cardiac myocytes
2013	[18]	Nanograin	60	30 (dia)	61	Au (200)	Si ₃ N ₄ (0.5)	Glass	(r/s) Rat neurons (h)
2013	[22]	CNT	64	50 (sq)	NA	ITO	acrylic imide	Glass	(r) Rat neurons (h)
2014	[55]	IrOx nanotube	64	34 μm^2	NA	Pt (80)	Si ₃ N ₄ /SiO ₂ (0.25/0.05)	Quartz	(r) Cardiac myocytes
2014	[107]	MWCNT	16	60 (dia)	NA	MWCNT	PDMS (150)	Medical tape	(r) Retinal slices
2014	[43]	Pt	NA	12 (dia)	200	Pt	ONONO (0.8)	Glass	(r) HL-1 cell
2014	[46]	Doped diamond	64	20 (dia)	NA	Doped diamond	SU-8(1.5)	Si wafer	(r) HL-1 cell

* (dia): diameter, (sq): square

** (r): recording, (s): electrical stimulation, (h): primary hippocampal culture, (c): primary cortical culture

imaging was used to study the electrical recording and stimulation of MEAs from cultured neurons [98]. Simultaneous recording of optical signals and electrical signals provided valuable information about the interpretation of calcium dye signals related with actual spiking timing. Optical stimulation can increase the resolution of neural stimulation. Optogenetics has been introduced to the cultured neurons to stimulate neurons that were not reachable through microelectrodes [99]. An optoelectronic device that integrated micropixelated InGaN light-emitting diode with microelectrode array was reported and tested with channel rhodopsin expressed HL-1

cells [100]. Although optogenetics are not fully deployed in combination with MEAs, there are large rooms for the development of opto-electrical MEA platform that will become an essential tool to interrogate *in vitro* neural circuits.

APPLICATIONS

Cell-based biosensors

Various chemicals have been tested to cultured neural network on MEAs in an attempt to quantitatively analyze the

MEA signals in accordance with chemical types and concentrations. Neurotransmitters or their blockers have been used to observe the network response. The effect of anandamide and methanandamide, which reversibly inhibit spike and burst production, was tested on cultured neural networks [101]. The synchronization activity of spinal cord was changed based on the concentration of bicuculline, strychnine, and 2,3-dioxo-6-nitro-1,2,3,4-tetrahydrobenzoquinoline-7-sulphonamide (NBQX) [102]. Robustness and reproducibility of neurotoxicity screening using MEA data have been reported [103].

A high-throughput platform is essential to deploy the MEA platform to drug-screening applications. Multi-well type MEA platforms were developed by a few vendors (*e.g.* Multi Channel Systems, Qwane Biosciences, Axion Biosystems). A micro-multiple well platform based on agarose microwell structures was proposed by Kang *et al.* [97]. A clustered neuronal network was formed in each microwell and a large number of repeating tests for an identical drug could be performed at once using the micro-well type MEA.

Testing platform for retinal prostheses

Researchers used MEAs to study the electrophysiological characteristics of retina slices, which is indispensable for developing retinal prosthetic devices. Various pulses, which were series of symmetric, anodic phase-first biphasic pulses with different amplitudes and pulse durations, were tested to search for efficient electrical stimulation protocols [104, 105]. Voltage controlled pulse stimulation was compared with current controlled pulse stimulation [104]. Chichilnisky and coworkers showed that multielectrode array with smaller electrode diameters (6 or 25 μm) and spacing (60 μm) could be used to stimulate retinal ganglion cells of mammalian retinal tissues, thus might be used for high-resolution retinal implant devices [105, 106]. Recently, Hanein and coworkers used the MEA technology to test a novel polymeric retinal implant platform based on a photo-sensitive bulk heterojunction layer (P3HT/N2200) [107].

SUMMARY

MEA is a versatile neural interface platform for *in vitro* neural tissues, which provides neural recording, electrical stimulation, and chemical stimulation. For past two decades, researchers made great effort to develop various types of MEAs that had more channels, durability, biocompatibility, functionality, and flexibility. Metal nanostructures, carbon nanotubes, conductive polymers, and nanowires showed great promise in enhancing the sensitivity of the MEA. State-of-the-art VLSI design technology has been used to increase the MEA channel capacity to a few thousands and

contributed to the miniaturization of the MEA system. MEA technology could be engineered to integrate microfluidic devices, optical interfaces, and surface micropatterning techniques. Microfluidic devices facilitated the study of neural information processing between two different neural populations. Surface micropatterning provided surface biofunctional schemes to MEAs. Finally, the MEA system has been utilized to numerous neural network studies and clinical applications such as drug screening, retinal slice studies, and neural network dynamic analysis. It is expected that the MEA technology will contribute to progress of network neuroscience.

ACKNOWLEDGEMENTS

This work was supported by the National Research Foundation of Korea grants (NRF-2012R1A2A1A01007327).

CONFLICT OF INTEREST STATEMENTS

Kim R declares that she has no conflict of interest in relation to the work in this article. Joo S declares that he has no conflict of interest in relation to the work in this article. Jung H declares that he has no conflict of interest in relation to the work in this article. Hong N declares that she has no conflict of interest in relation to the work in this article. Nam Y declares that he has no conflict of interest in relation to the work in this article.

REFERENCES

- [1] Thomas CA Jr, Springer PA, Loeb GE, Berwald-Netter Y, Okun LM. A miniature microelectrode array to monitor the bioelectric activity of cultured cells. *Exp Cell Res.* 1972; 74(1):61-6.
- [2] Pine J. Recording action potentials from cultured neurons with extracellular microcircuit electrodes. *J Neurosci Methods.* 1980; 2(1):19-31.
- [3] Gross GW. Simultaneous single unit recording *in vitro* with a photoetched laser deinsulated gold multimicroelectrode surface. *IEEE Trans Biomed Eng.* 1979; 26(5):273-9.
- [4] Novak JL, Wheeler BC. Recording from the *Aplysia* abdominal ganglion with a planar microelectrode array. *IEEE Trans Biomed Eng.* 1986; 33(2):196-202.
- [5] Boppart SA, Wheeler BC, Wallace CS. A flexible perforated microelectrode array for extended neural recordings. *IEEE Trans Biomed Eng.* 1992; 39(1):37-42.
- [6] Fromherz P. Electrical interfacing of nerve cells and semiconductor chips. *ChemPhysChem.* 2002; 3(3):276-84.
- [7] Stett A, Egert U, Guenther E, Hofmann F, Meyer T, Nisch W, Haemmerle H. Biological application of microelectrode arrays in drug discovery and basic research. *Anal Bioanal Chem.* 2003; 377(3):486-95.

- [8] Fromherz P, Offenhausser A, Vetter T, Weis J. A neuron-silicon junction: a Retzius cell of the leech on an insulated-gate field-effect transistor. *Science*. 1991; 252(5010):1290-3.
- [9] Guo J, Yuan J, Chan M. Modeling of the cell-electrode interface noise for microelectrode arrays. *IEEE Trans Biomed Circuits Syst*. 2012; 6(6):605-13.
- [10] Spira ME, Hai A. Multi-electrode array technologies for neuroscience and cardiology. *Nat Nanotechnol*. 2013; 8(2):83-94.
- [11] Buitengeweg JR, Rutten WL, Marani E. Modeled channel distributions explain extracellular recordings from cultured neurons sealed to microelectrodes. *IEEE Trans Biomed Eng*. 2002; 49(12 Pt 2):1580-90.
- [12] Cohen A, Shappir J, Yitzchaik S, Spira ME. Reversible transition of extracellular field potential recordings to intracellular recordings of action potentials generated by neurons grown on transistors. *Biosens Bioelectron*. 2008; 23(6):811-9.
- [13] Hai A, Shappir J, Spira ME. In-cell recordings by extracellular microelectrodes. *Nat Methods*. 2010; 7(3):200-2.
- [14] Buitengeweg JR, Rutten WL, Marani E. Extracellular stimulation window explained by a geometry-based model of the neuron-electrode contact. *IEEE Trans Biomed Eng*. 2002; 49(12 Pt 2):1591-9.
- [15] Chang JC, Brewer GJ, Wheeler BC. Microelectrode array recordings of patterned hippocampal neurons for four weeks. *Biomed Microdevices*. 2000; 2(4):245-53.
- [16] Nam Y, Chang JC, Wheeler BC, Brewer GJ. Gold-coated microelectrode array with thiol linked self-assembled monolayers for engineering neuronal cultures. *IEEE Trans Biomed Eng*. 2004; 51(1):158-65.
- [17] Xie C, Lin Z, Hanson L, Cui Y, Cui B. Intracellular recording of action potentials by nanopillar electroporation. *Nat Nanotechnol*. 2012; 7(3):185-90.
- [18] Kim R, Hong N, Nam Y. Gold nanograin microelectrodes for neuroelectronic interfaces. *Biotechnol J*. 2013; 8(2):206-14.
- [19] Kim JH, Kang G, Nam Y, Choi YK. Surface-modified microelectrode array with flake nanostructure for neural recording and stimulation. *Nanotechnology*. 2010; 21(8):85303.
- [20] Seker E, Berdichevsky Y, Begley MR, Reed ML, Staley KJ, Yarmush ML. The fabrication of low-impedance nanoporous gold multiple-electrode arrays for neural electrophysiology studies. *Nanotechnology*. 2010; 21(12):125504.
- [21] Wang K, Fishman HA, Dai H, Harris JS. Neural stimulation with a carbon nanotube microelectrode array. *Nano Lett*. 2006; 6(9):2043-8.
- [22] Suzuki I, Fukuda M, Shirakawa K, Jiko H, Gotoh M. Carbon nanotube multi-electrode array chips for noninvasive real-time measurement of dopamine, action potentials, and postsynaptic potentials. *Biosens Bioelectron*. 2013; 49:270-5.
- [23] Mathieson K, Kachiguine S, Adams C, Cunningham W, Gunning D, O'Shea V, Smith KM, Chichilnisky EJ, Litke AM, Sher A, Rahman M. Large-area microelectrode arrays for recording of neural signals. *IEEE Trans Nucl Sci*. 2004; 51(5):2027-31.
- [24] Egert U, Schlosshauer B, Fennrich S, Nisch W, Fejtł M, Knott T, Müller T, Hammerle H. A novel organotypic long-term culture of the rat hippocampus on substrate-integrated multielectrode arrays. *Brain Res Brain Res Protoc*. 1998; 2(4):229-42.
- [25] Prohaska OJ, Olcaytug F, Pfundner P, Dragaun H. Thin-film multiple electrode probes: Possibilities and limitations. *IEEE Trans Biomed Eng*. 1986; 33(2):223-9.
- [26] Gabay T, Ben-David M, Kalifa I, Sorkin R, Abrams ZR, Ben-Jacob E, Hanein Y. Electro-chemical and biological properties of carbon nanotube based multi-electrode arrays. *Nanotechnology*. 2007; 18(3):035201.
- [27] Bruggemann D, Wolfrum B, Maybeck V, Mourzina Y, Jansen M, Offenhausser A. Nanostructured gold microelectrodes for extracellular recording from electrogenic cells. *Nanotechnology*. 2011; 22(26):265104.
- [28] Drake KL, Wise KD, Farraye J, Anderson DJ, BeMent SL. Performance of planar multisite microprobes in recording extracellular single-unit intracortical activity. *IEEE Trans Biomed Eng*. 1988; 35(9):719-32.
- [29] Jun SB, Hynd MR, Dowell-Mesfin N, Smith KL, Turner JN, Shain W, Kim SJ. Low-density neuronal networks cultured using patterned poly-L-lysine on microelectrode arrays. *J Neurosci Methods*. 2007; 160(2):317-26.
- [30] Gross GW, Wen WY, Lin JW. Transparent indium-tin oxide electrode patterns for extracellular, multisite recording in neuronal cultures. *J Neurosci Methods*. 1985; 15(3):243-52.
- [31] Heuschkel MO, Fejtł M, Raggenbass M, Bertrand D, Renaud P. A three-dimensional multi-electrode array for multi-site stimulation and recording in acute brain slices. *J Neurosci Methods*. 2002; 114(2):135-48.
- [32] Oka H, Shimono K, Ogawa R, Sugihara H, Taketani M. A new planar multielectrode array for extracellular recording: application to hippocampal acute slice. *J Neurosci Methods*. 1999; 93(1):61-7.
- [33] Liang G, Guvanaseen GS, Xi L, Tuthill C, Nichols TR, DeWeerth SP. A PDMS-based integrated stretchable microelectrode array (isMEA) for neural and muscular surface interfacing. *IEEE Trans Biomed Circuits Syst*. 2013; 7(1):1-10.
- [34] Nam Y, Musick K, Wheeler BC. Application of a PDMS microstencil as a replaceable insulator toward a single-use planar microelectrode array. *Biomed Microdevices*. 2006; 8(4):375-81.
- [35] Blau A, Murr A, Wolff S, Semagor E, Medini P, Iurilli G, Ziegler C, Benfenati F. Flexible, all-polymer microelectrode arrays for the capture of cardiac and neuronal signals. *Biomaterials*. 2011; 32(7):1778-86.
- [36] Yu F, Zhao Y, Gu J, Quigley KL, Chi NC, Tai YC, Hsiai TK. Flexible microelectrode arrays to interface epicardial electrical signals with intracardial calcium transients in zebrafish hearts. *Biomed Microdevices*. 2012; 14(2):357-66.
- [37] Potter SM, DeMarse TB. A new approach to neural cell culture for long-term studies. *J Neurosci Methods*. 2001; 110(1-2):17-24.
- [38] Goyal G, Nam Y. Neuronal micro-culture engineering by microchannel devices of cellular scale dimensions. *Biomed Eng Lett*. 2011; 1(2):89-98.
- [39] Gesteland RC, Howland B, Lettvin JY, Pitts WH. Comments on Microelectrodes. *Proc IRE*. 1959; 47(11):1856-62.
- [40] Maher MP, Pine J, Wright J, Tai YC. The neurochip: a new multielectrode device for stimulating and recording from cultured neurons. *J Neurosci Methods*. 1999; 87(1):45-56.
- [41] Park S, Song YJ, Boo H, Chung TD. Nanoporous Pt microelectrode for neural stimulation and recording: *In vitro* characterization. *J Phys Chem C*. 2010; 114(19):8721-6.
- [42] Cui XY, Martin DC. Fuzzy gold electrodes for lowering impedance and improving adhesion with electrodeposited conducting polymer films. *Sensor Actuat A Phys*. 2003; 103(3):384-94.
- [43] Czeschik A, Offenhausser A, Wolfrum B. Fabrication of MEA-based nanocavity sensor arrays for extracellular recording of action potentials. *Phy Status Solidi A*. 2014; 211(6):1462-6.
- [44] Keefer EW, Botterman BR, Romero MI, Rossi AF, Gross GW. Carbon nanotube coating improves neuronal recordings. *Nat Nanotechnol*. 2008; 3(7):434-9.
- [45] Fuchsberger K, Le Goff A, Gambazzi L, Toma FM, Goldoni A, Giugliano M, Stelzle M, Prato M. Multiwalled carbon-

- nanotube-functionalized microelectrode arrays fabricated by microcontact printing: platform for studying chemical and electrical neuronal signaling. *Small*. 2011; 7(4):524-30.
- [46] Maybeck V, Edgington R, Bongrain A, Welch JO, Scorsone E, Bergonzo P, Jackman RB, Offenhausser A. Boron-doped nanocrystalline diamond microelectrode arrays monitor cardiac action potentials. *Adv Healthc Mater*. 2014; 3(2):283-9.
- [47] Cui X, Lee VA, Raphael Y, Wiler JA, Hetke JF, Anderson DJ, Martin DC. Surface modification of neural recording electrodes with conducting polymer/biomolecule blends. *J Biomed Mater Res*. 2001; 56(2):261-72.
- [48] Ludwig KA, Langhals NB, Joseph MD, Richardson-Burns SM, Hendricks JL, Kipke DR. Poly(3,4-ethylenedioxythiophene) (PEDOT) polymer coatings facilitate smaller neural recording electrodes. *J Neural Eng*. 2011; 8(1):014001.
- [49] Venkatraman S, Hendricks J, King ZA, Sereno AJ, Richardson-Burns S, Martin D, Carmena JM. *In vitro* and *in vivo* evaluation of PEDOT microelectrodes for neural stimulation and recording. *IEEE Trans Neural Syst Rehabil Eng*. 2011; 19(3):307-16.
- [50] Gerwig R, Fuchsberger K, Schroepel B, Link GS, Heusel G, Kraushaar U, Schuhmann W, Stett A, Stelzle M. PEDOT-CNT composite microelectrodes for recording and electrostimulation applications: Fabrication, morphology, and electrical properties. *Front Neuroeng*. 2012; 5:8.
- [51] Zhou H, Cheng X, Rao L, Li T, Duan YY. Poly(3,4-ethylenedioxythiophene)/multiwall carbon nanotube composite coatings for improving the stability of microelectrodes in neural prostheses applications. *Acta Biomater*. 2013; 9(5):6439-49.
- [52] Deng M, Yang X, Silke M, Qiu W, Xu M, Borghs G, Chen H. Electrochemical deposition of polypyrrole/graphene oxide composite on microelectrodes towards tuning the electrochemical properties of neural probes. *Sensor Actuat B Chem*. 2011; 158(1):176-84.
- [53] Kim W, Ng JK, Kunitake ME, Conklin BR, Yang P. Interfacing silicon nanowires with mammalian cells. *J Am Chem Soc*. 2007; 129(23):7228-9.
- [54] Robinson JT, Jorgolli M, Shalek AK, Yoon MH, Gertner RS, Park H. Vertical nanowire electrode arrays as a scalable platform for intracellular interfacing to neuronal circuits. *Nat Nanotechnol*. 2012; 7(3):180-4.
- [55] Lin ZC, Xie C, Osakada Y, Cui Y, Cui B. Iridium oxide nanotube electrodes for sensitive and prolonged intracellular measurement of action potentials. *Nat Commun*. 2014; 5:3206.
- [56] Nam Y, Branch DW, Wheeler BC. Epoxy-silane linking of biomolecules is simple and effective for patterning neuronal cultures. *Biosens Bioelectron*. 2006; 22(5):589-97.
- [57] Kang K, Lee S, Kim R, Choi IS, Nam Y. Electrochemically driven, electrode-addressable formation of functionalized polydopamine films for neural interfaces. *Angew Chem Int Ed Engl*. 2012; 51(52):13101-4.
- [58] Eversmann B, Jenkner M, Hofmann F, Paulus C, Brederlow R, Holzapfl B, Fromherz P, Merz M, Brenner M, Schreiter M, Gabl R, Plehnert K, Steinhäuser M, Eckstein G, Schmitt-Landsiedel D, Thewes R. A 128 × 128 CMOS biosensor array for extracellular recording of neural activity. *IEEE J Solid-State Circuits*. 2003; 38(12):2306-17.
- [59] Lambacher A, Vitzthum V, Zeitler R, Eickenscheidt M, Eversmann B, Thewes R, Fromherz P. Identifying firing mammalian neurons in networks with high-resolution multi-transistor array (MTA). *Appl Phys A-Mater*. 2011; 102(1):1-11.
- [60] Zeck G, Lambacher A, Fromherz P. Axonal transmission in the retina introduces a small dispersion of relative timing in the ganglion cell population response. *PLoS One*. 2011; 6(6):e20810.
- [61] Eickenscheidt M, Jenkner M, Thewes R, Fromherz P, Zeck G. Electrical stimulation of retinal neurons in epiretinal and subretinal configuration using a multicapacitor array. *J Neurophysiol*. 2012; 107(10):2742-55.
- [62] Berdondini L, Imfeld K, Maccione A, Tedesco M, Neukom S, Koudelka-Hep M, Martinoia S. Active pixel sensor array for high spatio-temporal resolution electrophysiological recordings from single cell to large scale neuronal networks. *Lab Chip*. 2009; 9(18):2644-51.
- [63] Imfeld K, Neukom S, Maccione A, Bornat Y, Martinoia S, Farine PA, Koudelka-Hep M, Berdondini L. Large-scale, high-resolution data acquisition system for extracellular recording of electrophysiological activity. *IEEE Trans Biomed Eng*. 2008; 55(8):2064-73.
- [64] Berdondini L, van der Wal PD, de Rooij NF, Koudelka-Hep M. Development of an electrodeless post-processing technique for depositing gold as electrode material on CMOS devices. *Sensor Actuat B Chem*. 2004; 99(2-3):505-10.
- [65] Ferrea E, Maccione A, Medrihan L, Nieuw T, Ghezzi D, Baldelli P, Benfenati F, Berdondini L. Large-scale, high-resolution electrophysiological imaging of field potentials in brain slices with microelectronic multielectrode arrays. *Front Neural Circuits*. 2012; 6:80.
- [66] Maccione A, Hennig MH, Gandolfo M, Muthmann O, van Coppenhagen J, Eglén SJ, Berdondini L, Sernagor E. Following the ontogeny of retinal waves: pan-retinal recordings of population dynamics in the neonatal mouse. *J Physiol*. 2014; 592(Pt 7):1545-63.
- [67] Frey U, Sedivy J, Heer F, Pedron R, Ballini M, Mueller J, Bakkum D, Hafizovic S, Faraci FD, Greve F, Kirstein K-U, Hierlemann A. Switch-matrix-based high-density microelectrode array in CMOS technology. *IEEE J Solid-St Circ*. 2010; 45(2):467-82.
- [68] Frey U, Egert U, Heer F, Hafizovic S, Hierlemann A. Microelectronic system for high-resolution mapping of extracellular electric fields applied to brain slices. *Biosens Bioelectron*. 2009; 24(7):2191-8.
- [69] Müller J, Bakkum DJ, Hierlemann A. Sub-millisecond closed-loop feedback stimulation between arbitrary sets of individual neurons. *Front Neural Circuits*. 2013; 6:121.
- [70] Bakkum DJ, Frey U, Radivojevic M, Russell TL, Müller J, Fiscella M, Takahashi H, Hierlemann A. Tracking axonal action potential propagation on a high-density microelectrode array across hundreds of sites. *Nat Commun*. 2013; 4:2181.
- [71] Ballini M, Müller J, Livi P, Chen Y, Frey U, Shadmani A, Jones IL, Gong W, Fiscella M, Radivojevic M, Bakkum D, Stett A, Heer F, Hierlemann A. A 1024-channel CMOS microelectrode-array system with 26'400 electrodes for recording and stimulation of electro-active cells in-vitro. *VLSI Circuits (VLSIC), 2013 Symposium on; 2013: IEEE; C54-C5*.
- [72] Park JW, Kim HJ, Kang MW, Jeon NL. Advances in microfluidics-based experimental methods for neuroscience research. *Lab Chip*. 2013; 13(4):509-21.
- [73] Taylor AM, Blurton-Jones M, Rhee SW, Cribbs DH, Cotman CW, Jeon NL. A microfluidic culture platform for CNS axonal injury, regeneration and transport. *Nat Methods*. 2005; 2(8):599-605.
- [74] Campenot RB. Local control of neurite development by nerve growth factor. *Proc Natl Acad Sci USA*. 1977; 74(10):4516-9.
- [75] Park J, Koito H, Li J, Han A. Multi-compartment neuron-glia co-culture platform for localized CNS axon-glia interaction study. *Lab Chip*. 2012; 12(18):3296-304.
- [76] Peyrin JM, Deleglise B, Saias L, Vignes M, Gougis P, Magnifico S, Betuing S, Pietri M, Caboche J, Vanhoutte P, Viovy JL, Brugg B. Axon diodes for the reconstruction of oriented neuronal networks in microfluidic chambers. *Lab*

- Chip. 2011; 11(21):3663-73.
- [77] Dworak BJ, Wheeler BC. Novel MEA platform with PDMS microtunnels enables the detection of action potential propagation from isolated axons in culture. *Lab Chip*. 2009; 9(3):404-10.
- [78] Morales R, Riss M, Wang L, Gavin R, Del Rio JA, Alcubilla R, Claverol-Tinture E. Integrating multi-unit electrophysiology and plastic culture dishes for network neuroscience. *Lab Chip*. 2008; 8(11):1896-905.
- [79] Pan L, Alagapan S, Franca E, Brewer GJ, Wheeler BC. Propagation of action potential activity in a predefined microtunnel neural network. *J Neural Eng*. 2011; 8(4):046031.
- [80] Brewer GJ, Boehler MD, Leondopulos S, Pan L, Alagapan S, DeMarse TB, Wheeler BC. Toward a self-wired active reconstruction of the hippocampal trisynaptic loop: DG-CA3. *Front Neural Circuits*. 2013; 7:165.
- [81] Honegger T, Scott MA, Yanik MF, Voldman J. Electrokinetic confinement of axonal growth for dynamically configurable neural networks. *Lab Chip*. 2013; 13(4):589-98.
- [82] Kanagasabapathi TT, Franco M, Barone RA, Martinoia S, Wadman WJ, Decre MM. Selective pharmacological manipulation of cortical-thalamic co-cultures in a dual-compartment device. *J Neurosci Methods*. 2013; 214(1):1-8.
- [83] Kanagasabapathi TT, Ciliberti D, Martinoia S, Wadman WJ, Decre MM. Dual-compartment neurofluidic system for electrophysiological measurements in physically segregated and functionally connected neuronal cell culture. *Front Neuroeng*. 2011; 4:13.
- [84] Takayama Y, Moriguchi H, Kotani K, Suzuki T, Mabuchi K, Jimbo Y. Network-wide integration of stem cell-derived neurons and mouse cortical neurons using microfabricated co-culture devices. *Biosystems*. 2012; 107(1):1-8.
- [85] Wheeler BC, Brewer GJ. Designing neural networks in culture: Experiments are described for controlled growth, of nerve cells taken from rats, in predesigned geometrical patterns on laboratory culture dishes. *Proc IEEE Inst Electr Electron Eng*. 2010; 98(3):398-406.
- [86] Chang JC, Brewer GJ, Wheeler BC. Modulation of neural network activity by patterning. *Biosens Bioelectron*. 2001; 16(7-8):527-33.
- [87] Segev R, Benveniste M, Hulata E, Cohen N, Palevski A, Kapon E, Shapira Y, Ben-Jacob E. Long term behavior of lithographically prepared *in vitro* neuronal networks. *Phys Rev Lett*. 2002; 88(11):118102.
- [88] Cheng J, Zhu G, Wu L, Du X, Zhang H, Wolfrum B, Jin Q, Zhao J, Offenhausser A, Xu Y. Photopatterning of self-assembled poly (ethylene) glycol monolayer for neuronal network fabrication. *J Neurosci Methods*. 2013; 213(2):196-203.
- [89] Boehler MD, Leondopulos SS, Wheeler BC, Brewer GJ. Hippocampal networks on reliable patterned substrates. *J Neurosci Methods*. 2012; 203(2):344-53.
- [90] James CD, Spence AJ, Dowell-Mesfin NM, Hussain RJ, Smith KL, Craighead HG, Isaacson MS, Shain W, Turner JN. Extracellular recordings from patterned neuronal networks using planar microelectrode arrays. *IEEE Trans Biomed Eng*. 2004; 51(9):1640-8.
- [91] Jungblut M, Knoll W, Thielemann C, Pottek M. Triangular neuronal networks on microelectrode arrays: an approach to improve the properties of low-density networks for extracellular recording. *Biomed Microdevices*. 2009; 11(6):1269-78.
- [92] Marconi E, Nieuws T, Maccione A, Valente P, Simi A, Messa M, Dante S, Baldelli P, Berdondini L, Benfenati F. Emergent functional properties of neuronal networks with controlled topology. *PLoS One*. 2012; 7(4):e34648.
- [93] Kang K, Choi IS, Nam Y. A biofunctionalization scheme for neural interfaces using polydopamine polymer. *Biomaterials*. 2011; 32(27):6374-80.
- [94] Suzuki M, Ikeda K, Yamaguchi M, Kudoh SN, Yokoyama K, Satoh R, Ito D, Nagayama M, Uchida T, Gohara K. Neuronal cell patterning on a multi-electrode array for a network analysis platform. *Biomaterials*. 2013; 34(21):5210-7.
- [95] Jimbo Y, Robinson HP, Kawana A. Simultaneous measurement of intracellular calcium and electrical activity from patterned neural networks in culture. *IEEE Trans Biomed Eng*. 1993; 40(8):804-10.
- [96] Suzuki I, Sugio Y, Jimbo Y, Yasuda K. Stepwise pattern modification of neuronal network in photo-thermally-etched agarose architecture on multi-electrode array chip for individual-cell-based electrophysiological measurement. *Lab Chip*. 2005; 5(3):241-7.
- [97] Kang G, Lee JH, Lee CS, Nam Y. Agarose microwell based neuronal micro-circuit arrays on microelectrode arrays for high throughput drug testing. *Lab Chip*. 2009; 9(22):3236-42.
- [98] Herzog N, Shein-Idelson M, Hanein Y. Optical validation of *in vitro* extra-cellular neuronal recordings. *J Neural Eng*. 2011; 8(5):056008.
- [99] Tchumatchenko T, Newman JP, Fong MF, Potter SM. Delivery of continuously-varying stimuli using channelrhodopsin-2. *Front Neural Circuits*. 2013; 7:184.
- [100] Yakushenko A, Gong Z, Maybeck V, Hofmann B, Gu E, Dawson M, Offenhausser A, Wolfrum B. On-chip optical stimulation and electrical recording from cells. *J Biomed Opt*. 2013; 18(11):111402.
- [101] Morefield SI, Keefer EW, Chapman KD, Gross GW. Drug evaluations using neuronal networks cultured on microelectrode arrays. *Biosens Bioelectron*. 2000; 15(7-8):383-96.
- [102] Selinger JV, Pancrazio JJ, Gross GW. Measuring synchronization in neuronal networks for biosensor applications. *Biosens Bioelectron*. 2004; 19(7):675-83.
- [103] Novellino A, Scelfo B, Palosaari T, Price A, Sobanski T, Shafer TJ, Johnstone AF, Gross GW, Gramowski A, Schroeder O, Jugelt K, Chiappalone M, Benfenati F, Martinoia S, Tedesco MT, Defranchi E, D'Angelo P, Whelan M. Development of micro-electrode array based tests for neurotoxicity: assessment of interlaboratory reproducibility with neuroactive chemicals. *Front Neuroeng*. 2011; 4:4.
- [104] Goo YS, Ye JH, Lee S, Nam Y, Ryu SB, Kim KH. Retinal ganglion cell responses to voltage and current stimulation in wild-type and rd1 mouse retinas. *J Neural Eng*. 2011; 8(3):035003.
- [105] Sekirnjak C, Hottowy P, Sher A, Dabrowski W, Litke AM, Chichilnisky EJ. Electrical stimulation of mammalian retinal ganglion cells with multielectrode arrays. *J Neurophysiol*. 2006; 95(6):3311-27.
- [106] Sekirnjak C, Hottowy P, Sher A, Dabrowski W, Litke AM, Chichilnisky EJ. High-resolution electrical stimulation of primate retina for epiretinal implant design. *J Neurosci*. 2008; 28(17):4446-56.
- [107] Gautam V, Rand D, Hanein Y, Narayan KS. A polymer optoelectronic interface provides visual cues to a blind retina. *Adv Mater*. 2014; 26(11):1751-6.
- [108] Lambacher A, Jenkner M, Merz M, Eversmann B, Kaul RA, Hofmann F, Thewes R, Fromherz P. Electrical imaging of neuronal activity by multi-transistor-array (MTA) recording at 7.8 μm resolution. *Appl Phys A*. 2004; 79(7):1607-11.